Published in final edited form as:
Prostate. 2014 February ; 74(2): 187–200. doi:10.1002/pros.22740.

Enrichment of human prostate cancer cells with tumor initiating properties in mouse and zebrafish xenografts by differential adhesion

Nitu Bansal[1], **Stephani Davis**[2], **Irina Tereshchenko**[1], **Tulin Budak-Alpdogan**[1], **Hua Zhong**[3], **Mark N. Stein**[1,4], **Isaac Yi Kim**[1,5], **Robert S. DiPaola**[1,4], **Joseph R. Bertino**[1,2,4,*], and **Hatem E. Sabaawy**[1,2,4,*]

[1]Rutgers Cancer Institute of New Jersey, 195 Little Albany Street, New Brunswick, NJ 08903-2681

[2]Department of Pharmacology, Rutgers-Robert Wood Johnson Medical School, New Brunswick, NJ 08903-2681

[3]Department of Pathology and Laboratory Medicine, Rutgers-Robert Wood Johnson Medical School, New Brunswick, NJ 08903-2681

[4]Department of Medicine, Rutgers-Robert Wood Johnson Medical School, New Brunswick, NJ 08903-2681

[5]Department of Surgery, Rutgers-Robert Wood Johnson Medical School, New Brunswick, NJ 08903-2681

Abstract

BACKGROUND—Prostate tumor-initiating cells (TICs) have intrinsic resistance to current therapies. TICs are commonly isolated by cell sorting or dye exclusion, however, isolating TICs from limited primary prostate cancer (PCa) tissues is inherently inefficient. We adapted the collagen adherence feature to develop a combined immunophenotypic and time-of-adherence assay to identify human prostate TICs.

METHODS—PCa cells from multiple cell lines and primary tissues were allowed to adhere to several matrix molecules, and fractions of adherent cells were examined for their TIC properties.

RESULTS—Collagen-I rapidly-adherent PCa cells have significantly higher clonogenic, migration, and invasion abilities, and initiated more tumor xenografts in mice when compared to slowly-adherent and no-adherent cells. To determine the relative frequency of TICs among PCa

[*]Corresponding authors: J. R. Bertino, M.D., Rutgers Cancer Institute of New Jersey, 195 Little Albany Street, Room 3033, New Brunswick, NJ 08903-2681, USA. Telephone: 732-235-8510, bertinoj@umdnj.edu. H. E. Sabaawy, M.D., Ph.D., Rutgers Cancer Institute of New Jersey, 195 Little Albany Street, Room 4557, New Brunswick, NJ 08903-2681, USA. Telephone: 732-235-8081, sabaawhe@umdnj.edu.

AUTHORS CONTRIBUTIONS

1. Conception and design – Nitu Bansal, Hatem E. Sabaawy, Joseph R. Bertino.
2. Provision of study material or patient samples –Mark N. Stein, Hua Zhong, Isaac Yi Kim.
3. Collection and assembly of data – Nitu Bansal, Stephani Davis, Hatem E. Sabaawy.
4. Data analyses – Nitu Bansal, Irina Tereshchenko, Hatem E. Sabaawy, Robert DiPaola, Joseph R. Bertino.
5. Manuscript writing – Hatem E. Sabaawy, Joseph R. Bertino.

All authors declare no competing interest.

cell lines and primary PCa cells, we utilized zebrafish xenografts to define the tumor initiation potential of serial dilutions of rapidly-adherent $\alpha2\beta1^{hi}/CD44^{hi}$ cells compared to non-adherent cells with $\alpha2\beta1^{low}/CD44^{low}$ phenotype. Tumor initiation from rapidly-adherent $\alpha2\beta1^{hi}/CD44^{hi}$ TICs harboring the TMPRSS2:ERG fusion generated xenografts comprising of PCa cells expressing Erg, AMACR, and PSA. Moreover, PCa-cell dissemination was consistently observed in the immune-permissive zebrafish microenvironment from as-few-as 3 rapidly-adherent $\alpha2\beta1^{hi}/CD44^{hi}$ cells. In zebrafish xenografts, self-renewing prostate TICs comprise 0.02–0.9% of PC3 cells, 0.3–1.3% of DU145 cells, and 0.22–14.3% of primary prostate adenocarcinomas.

CONCLUSION—Zebrafish PCa xenografts were used to determine that the frequency of prostate TICs varies among PCa cell lines and primary PCa tissues. These data support a paradigm of utilizing zebrafish xenografts to evaluate novel therapies targeting tumor initiating cells in prostate cancer.

Keywords

Prostate cancer stem cells; tumor-initiating cells; zebrafish

INTRODUCTION

Prostate cancers were suggested to contain tumor cells that can self-renew, differentiate into multiple cell types reconstituting the diverse tumor population, and have enhanced proliferative capacity to drive the continued expansion of malignant cells [1]. These cells were identified as tumor-initiating cells (TICs) [2,3] that are able to form tumors in immune-compromised mice, and self-renew in serial transplantation studies [4]. Genetic and lineage tracing studies have recently provided substantial evidence that subpopulations of tumor cells or TICs direct tumor growth in mice [5–7]. These cells survive treatments by virtue of possessing anti-apoptotic signals, high levels of drug-efflux membrane transporters, and high DNA repair capacity [8]. Since TICs are commonly resistant to conventional chemotherapies, and prostate tumors develop resistance to hormonal ablation therapy [9], an attractive cancer treatment strategy is to identify TICs and then use agents that effectively target the self-renewal abilities of TICs, alone or in combination with hormone ablation as an initial therapy to accomplish total tumor eradication, and to reduce the risk of relapse and metastasis.

Prostate cancer (PCa) TICs showed enhanced expression of self-renewal and stem cell markers such as Bmi-1, Oct4, β-catenin, and SMO supporting the presence of prostate TICs with stem cell properties [10]. Moreover, knockdown of these self-renewal signals in metastatic PCa leads to tumor cell death [11]. Thus, development of methods to enrich for TICs would provide a platform for the identification and preclinical examination of novel therapies that target self-renewal signals in prostate TICs.

Prostate tumors contain several functionally diverse cell types including TICs that can be of basal and/or luminal origin(s) [12], transit amplifying cells, terminally differentiated cells, and supportive stromal cells. The fraction of cells with TIC abilities would likely vary among different PCa cell lines and primary patient samples; however, it is generally believed to be a smaller fraction of cells within each tumor. Therefore, isolating the TIC subpopulation from a limited number of fresh primary PCa cells for study and manipulation is inherently inefficient.

PCa cells were shown to harbor a series of TMPRSS2-Ets fusion proteins generated through chromosomal translocations [13], and detected using interphase fluorescent *in situ* hybridization (FISH) techniques. The TMPRSS2-Ets fusions frequently result in overexpression of Ets proteins such as Erg when PCa cells are examined with

immunohistochemistry (IHC), making overexpression of Erg as one of the most PCa-specific biomarkers yet identified [14]. Another biomarker is the overexpression of alpha-methylacyl coenzyme A racemase (AMACR), which in combination with absence of basal cell layer markers are typical phenotypes of acinar prostatic adenocarcinoma. Integrin-β I has also been recognized as a basal cell marker associated with certain stem cell properties, and has been used as a cell surface maker for enrichment of epidermal keratinocyte stem cells [15] and human prostate epithelial stem cells [16]. We attempted to enrich putative TICs from PCa cell lines and primary samples based on adhesion to collagen-I, collagen-VI, or laminin; that are all β1-Integrin ligands. We then examined their TIC properties *in vitro* and *in vivo* in mice and zebrafish xenografts.

Tumor cell xenografts in the teleost zebrafish (*Danio rerio*) might allow for monitoring of tumor initiation from a limited number of TICs, thus mimicking the orderly stages of tumor growth, relapse, and metastasis. The zebrafish xenograft model offers several advantages over traditional murine and chick embryo xenograft models. Zebrafish embryos are small, develop rapidly, and hundreds are produced daily from each pair, making zebrafish an excellent vertebrate tool for testing chemicals *in vivo*, and for cancer drug discovery [17]. The optical clarity of zebrafish embryos and Casper [18] adult fish allows for non-invasive observation of tumor initiation, migration, and metastasis [19–21]. Earlier TIC reports suggested that TICs from the same patient are more prevalent in the highly immune-permissive NOD-SCID-IL2Rγ deficient mice than in the NOD-SCID deficient mice [22]. In contrast, the use of zebrafish embryos in a pre-immune, more xenograft-tolerant, environment would be advantageous to determine the self-renewal potential of prostate TICs. Here, we demonstrate that a fraction of cells isolated from multiple PCa cell lines and primary cells have tumor initiation potential in mice and zebrafish. Moreover, we found that prostate TIC frequency of primary PCa cells is much higher than TIC frequency of cells from established PCa cell lines in zebrafish xenografts.

MATERIALS AND METHODS

Materials

Taxotere, doxorubicin, and methotrexate were from the Cancer Institute of New Jersey pharmacy. Both collagen-I, -IV and laminin were purchased from BD Biosciences, and athymic$^{nu/nu}$ mice were from Jackson laboratory.

Fresh human prostate cancer samples

PCa patients diagnosed at the CINJ between 2008 and 2012 were enrolled. Prostate TICs and populations lacking TICs were isolated and characterized from prostatectomy specimens. Informed consents were obtained. De-identified PCa specimens were collected under institutional review board (IRB)-approved protocol. We used samples with similar Gleason scores determined through the review of diagnostic pathology reports. Primary cells were isolated as described in supplementary methods, allowed to adhere to collagen-I, and subfractions were sorted and transplanted into fish embryos.

Cell lines culture, prostate spheres, colony formation, migration, and invasion assays

Prostate normal and cancer cells were maintained at low passage numbers and utilized for clonogenic, migration, invasion, and prostate sphere forming assays as described in supplementary methods and elsewhere [23–25].

Collagen adherence assay

Putative TICs were isolated by combining phenotypic analyses [3] with collagen-I adherence. In brief, tissue culture dishes were coated with 70 μg/ml of collagen-I for 1 hr at room temperature or overnight at 4°C. Plates were washed with PBS, blocked in 0.3% BSA for 30 minutes, washed again, and cells were plated on collagen-I for 5 or 20 min. Cells that adhere in 5 min, and cells that did not adhere after 20 min were collected, and used.

Flow cytometry, IHC, interphase FISH, a nd cytotoxicity assays

Prostate cells were analyzed using FACScan cytometer and CellQuest software (BD). Flow cytometry, IHC, interphase FISH for TMPRSS2:Erg fusions, and cytotoxicity assays were performed as described in supplementary methods. IC_{50} concentrations used in cytotoxicity assays are described in supplementary methods and supplementary Fig. 1D, and were determined using Hill's equation in Graph-Pad prism 4.0 software.

Xenograft studies in nude mice

Animals were used in accordance with an approved protocol from RWJMS. PCa cells, 5-min collagen-adherent, and 20 min-non-adherent cells were injected along with matrigel in a 1:1 ratio into the abdominal flanks of nude mice (n=8 mice/group). A subset of each cell population was analyzed for cell viability to confirm that viable cells were being injected into the mice. Every 3 days, tumor dimensions were measured using a Vernier caliper, and tumor volumes were calculated as described [26].

Labeling and transplantation of prostate cancer cells in zebrafish

Wild type EKK and AB* zebrafish (*Danio rerio*) were maintained following an approved animal protocol. Adult fish were spawned and reared in conditioned water at 28.5°C on a 14-h light-10-h dark cycle. Embryos were staged as described (http://zfin.org). To track human cells in embryos and juvenile Casper [18] fish, we labeled PCa cells with quantum dots (QDs) that are virtually resistant to photobleaching. PCa cells were resuspended in 0.5x Dulbecco's PBS (DPBS) containing QD605 (red fluorescence) (Invitrogen) and lipofectamine at a ratio of 1:2 for 2 hours. Cells in 0.5x DPBS were used for transplantation into dechorionated and anesthetized (0.5x tricaine methanesulfonate, MS-222; Sigma) 48-hour post fertilization (hpf) embryos using 15 μm (internal diameter) injection needles. Transplantation of fresh cells or cells dissociated from primary xenograft regions and sorted for serial transplantation were done as described in supplementary methods and as previously described [27]. Microinjections were either subcutaneously (SC), or above the yolk into the sinus venosus using a Celltram microinjector. After transplantation and initial imaging, embryos were incubated for 2 hours at 37°C, and were then maintained in a humidified incubator at 33–34°C for up to 12 days post transplantation (dpt). Human cells were monitored under fluorescent microscopy for homing and tissue repopulation.

Juvenile zebrafish at 6–8 weeks of age were immune-suppressed with 10 μg/ml dexamethazone for 2 days as previously described [19,28], and were also utilized to generate xenografts. Juvenile fish were monitored for tumor growth and metastasis for up to 5 weeks.

Extreme Limiting dilution analysis (ELDA)

ELDA was used to assess the number of self-renewing cells contained within the bulk of the primary PCa mass as described in supplementary methods. The TIC frequency was finally calculated after 12 dpt using a linear regression method that was completed using ELDA [29] at http://bioinf.wehi.edu.au/cgi-bin/limdil/limdil.pl.

Statistical Analysis

All experiments were performed thrice, and each experiment was done in triplicates. Statistical analyses were done using student's t-test unless otherwise indicated. Results are presented as mean ± standard deviation (SD). Limiting dilution analysis (LDA), ELDA [29], and L-Calc statistical software were used to determine the frequencies of self-renewing TICs. A p-value of <0.05 was considered significant.

RESULTS

Isolation and characterization of human prostate tumor-initiating cells

Several strategies have been proposed to isolate prostate TICs, including the use of a combination of unique surface markers. Phenotypic markers identified for prostate TICs are $CD44^{hi}$, $CD44^{+}/CD24^{-}$ [30], and $CD44^{hi}$, $\alpha2\beta1\text{-integrin}^{hi}$, and $CD133^{+}$ [3,16]. Trop2 marker has also been used in combination with $CD49f^{+}$ to enrich for sphere-forming cells from human prostate [31]. We elected to use a strategy of combining phenotypic and time-of-adherence assays to isolate TICs from PCa cells. The adhesion properties of prostate cancer cells were examined by incubating cells on either laminin, collagen-I, collagen-IV coated dishes, or when all three matrix molecules are combined for different lengths of time from 5, 10, 15, to 20 minutes. As seen in Fig. 1 for DU145 cells from six separate adhesion experiments, PCa cells rapidly adhered to collagen-I coated dishes within 5 min. The assay is based on the finding that epidermal and testicular stem cells express higher levels of $\alpha2\beta1$- and $\alpha3\beta1$-integrins than transit amplifying or differentiated cells [32,33]. To isolate putative TICs, PCa cells from four cell lines and six primary patient prostatectomies (Table 1) were plated on collagen-I-coated dishes for 5 minutes, and adherent cells were collected. Non-adherent cells were replated for 20 minutes. After 20 minutes, non-adherent cells were also collected. To investigate whether the rapidly collagen-adherent cells (at 5min) had increased expression of $\alpha2\beta1$-integrin positive cells (a marker for TICs), we performed flow cytometric analyses of the different fractions, and found that the rapidly adherent cells have higher $\alpha2\beta1$-integrin expression from both DU145 and PC3 cells (Fig. 1B) compared to the 20′ non-adherent cells. Differential adhesion was readily detectable when collagen-I was used (Fig. 1A), hence we performed further experiments utilizing collagen-I. Similar percentages of collagen-I adherent cells were seen from both DU145 and PC3 cells (Fig. 1C). To exclude that the differential adhesion of PCa cells to collagen-I coated dishes was due to differences in cell viability or interference with cell proliferation abilities, we compared the proliferation of the differentially adherent fractions to the non-selected ones, and found no significant difference in cell proliferation (Supplementary Fig. 1). Cell viabilities of adherent and non-adherent cells immediately after cell isolation were similar (Fig. 1D) and were on average 95–99.9%. We also found that the rapidly adherent cells retained a more cohesive colony-like morphology after plating for 6 days, while 20 min nonadherent and adherent cells retained a less cohesive and mixed morphology, respectively (Supplementary Fig. 1).

We then examined the expression of stem cell markers in DU145, PC3, LNCap, and CWR22 PCa cells. $CD44^{hi}$ and $\alpha2\beta1\text{-integrin}^{hi}$ cells were detected in all four cell lines (Fig. 2A), while CD133 expression was very low ($\leq0.01\%$) to not detectable. We isolated TICs from these prostate cancer cell lines by combining phenotypic selection with collagen-I adherence. The 5 min-adherent cell fraction comprised on average 4–6% of DU145 and PC3 cells, but was 2–3 fold less in both LNCap and CWR22 cells (Fig. 2B). Expression of CD44, $\alpha2\beta1$-integrin, and CD133 in each fraction was analyzed. The 5 min-adherent cell fraction had an average of several fold higher number of cells highly coexpressing $\alpha2\beta1$ and CD44 as compared to the 20 min-non-adherent fractions in all of the PCa cells examined (Fig. 2B and Supplementary Fig. 2A). Thus phenotypically, the 5 min-adherent fraction is enriched in

$\alpha2\beta1^{hi}/CD44^{hi}$ cells, while the 20 min-non-adherent fraction comprise $\alpha2\beta1^{low}/CD44^{low}$ cells. When cells from the 5 min-adherent fraction of PC3 and DU145 cells that are $\alpha2\beta1^{hi}/CD44^{hi}$ cells were grown as prostate spheres, known to contain putative TICs that can initiate serially passageable spheres, the consistently low CD133 expression increased, and up to 5% of the cells were $CD133^{+}$ (Fig. 2D). Significant upregulation of CD133 expression was detected in spheres of DU145 and PC3 cells (Fig. 2D) and CWR22 cells (Supplementary Fig. 2C), while CD133 was still undetectable in LNCap cells when grown as prostate spheres.

To examine if combining phenotypic and time-of-adherence assays could be used to isolate TICs from primary PCa cases (n=6), we collected fresh tissues from 6 matched PCa patients with similar Gleason scores (Table 1), and subjected them to the same assay. Similar to PCa cell lines, the 5 min-adherent fraction from primary samples was enriched in $\alpha2\beta1^{hi}/CD44^{hi}$cells, and in $CD133^{+}$ cells when grown as prostate spheres, compared to the non-adherent fraction (Fig. 2E).

Tumorigenic and self-renewal capacities of adherent tumor cells

To determine if the 5 min-adherent cell fraction contains TICs, $\alpha2\beta1^{hi}/CD44^{hi}$ DU145 cells within this fraction were examined by colony formation, and migration and invasion assays. The 5 min-adherent cell fraction with an $\alpha2\beta1^{hi}/CD44^{hi}$ phenotype showed a nearly 2-fold higher colony formation (Fig. 3A), and increased migration and invasion abilities as compared to $\alpha2\beta1^{low}/CD44^{low}$ cells (Fig. 3A). Similarly, PC3, CWR22 and LNCap cells within the 5 min-adherent cell fractions with an $\alpha2\beta1^{hi}/CD44^{hi}$ phenotype showed variable but consistently higher colony and spheroid formation abilities (Supplementary Fig. 2A–C). Since DU145 and PC3 cells displayed a larger 5 min-adherent cell fraction with an $\alpha2\beta1^{hi}/CD44^{hi}$ phenotype, we utilized these cells in most of our assays. An essential characteristic of TICs is their ability to self-renew in serial plating assays.

The $\alpha2\beta1^{hi}/CD44^{hi}$ DU145 cells formed significantly more single cell-derived spheroids as compared to $\alpha2\beta1^{low}/CD44^{low}$ cells. Moreover, spheroids formed from $\alpha2\beta1^{low}/CD44^{low}$ DU145 cells were fewer after day-5, and stopped growing after day-9 (Supplementary Fig. 3A, 3B) suggesting that these cells lack self-renewal abilities. To assess self-renewal at an earlier time point of sphere formation, single cells derived from day 7-primary spheroids were replated for secondary spheroid formation. Once again, $\alpha2\beta1^{hi}/CD44^{hi}$ DU145 cells generated significantly more spheroids than $\alpha2\beta1^{low}/CD44^{low}$ cells (Supplementary Fig. 3C). Therefore, the $\alpha2\beta1^{hi}/CD44^{hi}$ PCa cells exhibit enhanced tumorigenic, invasive, and self-renewal abilities.

Adherent cells are resistant to commonly used chemotherapeutic drugs

TICs were shown to be resistant to chemotherapies [34]. Since we isolated putative TICs by collagen adherence, we hypothesized that treatment with drugs that target TICs would reduce the number of cells adhering to collagen-I. Hence, we performed the collagen adherence assay upon treatment with chemotherapies commonly used for PCa at IC_{50s} established by MTS assays (Supplementary Fig. 3D). Indeed, the number of DU145 collagen-adherent cells was not affected by chemotherapy treatments, and on the contrary increased with methotrexate and carboplatin (Supplementary Fig. 3E) suggesting that these mainstream clinically used chemotherapeutic agents might increase the percentage of putative TICs.

Tumor initiation in nude mice

An essential property of TICs is their ability to initiate tumor growth in immune-compromised mice with limited cell numbers. We tested whether the 5 min-adherent DU145

cells are more tumorigenic than the non-adherent fraction. Cells were injected SC in the abdominal flanks of nude mice. Tumors were analyzed by three variables: tumor incidence, tumor growth rate (mm^3/day), and final tumor volume (mm^3; Fig. 3B–C). Only 17% of mice (n=3/20) injected with non-adherent cells developed tumors, while nearly all mice injected with either adherent (n=18/20) (90%) or total DU145 cells (n=17/20) (85%) developed tumors. Mice injected with adherent cells developed tumors as early as 15 days post-transplantation, compared to day 35 for mice injected with the same cell dose of one million total DU145 cells. In an additional experiment, injection of only 1,000 adherent cells resulted in tumor formation and tumor volumes that were significantly larger than those generated by injections of one million total DU145 cells (data not shown). After 50 days of growth, adherent DU145 tumors reached an average final volume of 867 mm^3. This was significantly larger than non-adherent and total DU145 tumors (Fig. 3B–C), which reached final volumes of 126 and 338 mm^3, with P values of 0.0006 and 0.0001, respectively when compared with adherent cell tumors. Thus, the $\alpha2\beta1^{hi}/CD44^{hi}$ DU145 cells are more tumorigenic in mice.

Evaluation of prostate TICs *in vivo* in zebrafish xenografts

To generate a PCa xenograft model in zebrafish for studying TICs, we employed a collagen adherence, cell sorting, and QD labeling strategy. Cells from PCa cell lines and primary samples were QD-labeled at near-100% efficiency (Fig. 4A–B). QD-labeled PCa cells, but not normal prostate epithelial cells, engrafted robustly in the pre-immune zebrafish embryos, and histological analyses demonstrated cells migrating to distal sites in zebrafish including muscle regions (Fig. 4C–D). Embryos with xenografts from the 5-min-adherent $\alpha2\beta1^{hi}/CD44^{hi}$ PCa cells displayed significantly shorter survival rates, and rapid death from tumor burden with a median survival of 100±19 hour post transplant (hpt), compared to median survivals of 108±10 hpt and 186±23 hpt for the parental DU145 and the $\alpha2\beta1^{low}/CD44^{low}$ cells, respectively (Fig. 4E) (n=200 embryo/group, $p<0.001$). Similar data were obtained from PC3, CWR22 and LNCap cells (Fig. 4E) as well as primary PCa cells (see below). The maximum tolerated cell doses for DU145, PC3 and primary PCa cell transplants ranged from 0.4 to 2 x 10^3 cells, which resulted in death from generalized tumor burden at 2–5 days post transplant (dpt) with PCa cells but not with immortalized normal prostate epithelial cells (RWPE-1) (Fig. 4E). QD-labeled parental cells, $\alpha2\beta1^{hi}/CD44^{hi}$ cells sorted from 5-min-adherent cells, and $\alpha2\beta1^{low}/CD44^{low}$ cells sorted from 20-min-non-adherent cells were transplanted at limiting dilution with cell doses from 1x10^3 to 3 cells either SC to allow for tumor cell dissemination or into the yolk of 48-hpf zebrafish embryos. We sorted embryos post-injection to ensure the placement and number of labeled cells, and grew the selected embryos at 33°C.

Transplanted cells and tumor growth were traceable *in vivo* in living fish (Fig. 5A). QD-labeled primary PCa cells (Fig. 5A) or DU145 cells (Fig. 5B–E) developed xenografts in zebrafish embryos. DU145 cells injected SC formed localized tumor xenografts at 4 dpt (Fig. 5B) that frequently migrated throughout the zebrafish muscle tissues, and often spread causing brain metastasis (Fig. 5D–E, left arrow), exophthalmus (Fig. 5D, arrowheads) (Supplementary Table 1), and death from disseminated tumor burden within 9 dpt. Cells in xenografts derived from adherent $\alpha2\beta1^{hi}/CD44^{hi}$ (TICs) disseminated to the brain region of zebrafish embryos, and were detected using IHC with the human-specific CD44 isoform (Fig. 5I). The overall rates of tumor formation from DU145 cells injected SC and in the yolk of embryonic zebrafish were 35.6% (n=57/160) for parental cells, 12.8% (n=22/171) for $\alpha2\beta1^{low}/CD44^{low}$ non-adherent (Non-TICs) cells, but significantly higher at 58.7% (n=98/167) for adherent $\alpha2\beta1^{hi}/CD44^{hi}$ (TICs) cells ($p<0.001$) (Supplementary Table 1). SC injections yielded an overall higher tumor formation rates than yolk transplants (Supplementary Table 1). Disseminated colonies of QD-labeled cells at >5 distant sites were

identified at a significantly higher frequencies in xenografts from TICs than from parental or non-TICs. Dissemination rates of SC or into yolk injections were 69%, 39% in 10-parental-cell-, and 26%, 29% in 3-parental-cell-transplants, were 21%, 9% in 10-cell-non-TICs and 17%, 10% for 3-cell-non-TICs transplants, and were 80%, 55% for 10-TIC, and 49%, 52% for 3-TIC-transplants (Supplementary Table 1). Similar results were obtained with PC3, CWR22, LNCap PCa cells. Moreover, PC3 adherent $\alpha2\beta1^{low}/CD44^{low}$ cells showed a significantly higher tumor initiation potential than PC3 non-TICs (Supplementary Table S2), suggesting that collagen adhesion might enrich for TICs with added phenotypes to $\alpha2\beta1$/CD44 expression.

We next isolated TICs from primary prostate cancers to examine their ability to initiate zebrafish xenografts similar to PCa cell lines. Prostate cancers used were diagnosed based on histological examination of H&E stained slides (Supplementary Fig. 4). To confirm that zebrafish xenografts were derived from PCa cells and not from benign or normal epithelial cells, we utilized the expression of AMACR and overexpression of Erg as prostate cancer-specific biomarkers [14]. We first optimized the detection of Erg and AMACR by IHC in PCa tissues (Supplementary Fig. 5). We then identified primary PCa cells harboring ERG gene rearrangements determined by interphase FISH (Supplementary Fig. 6), and examined Erg expression in the mirror sections of sampled PCa tissue and after formation of fish xenografts.

Indeed, tumor cells in the mirror section (Fig. 5J, and Supplementary Fig. 5–6) and zebrafish xenografts (Fig. 5K) showed strong immunoreactivity with antibodies against AMACR and Erg, suggesting that these zebrafish xenografts are derived from PCa cells. Further analysis of human PCa cells in xenografts derived from adherent $\alpha2\beta1^{hi}/CD44^{hi}$ (TICs) that frequently disseminated to the brain region of zebrafish embryos (Fig. 5H–I), or migrated to the tail (Supplementary Fig. 7A–D) demonstrated that many (but not all) of these cells were positive for CD44 expression (evidence for formation of $CD44^{-}$ cells, or CD44 plasticity), and demonstrated features of potential cell differentiation including the expression of CK8/18 (Supplementary Fig. 7C–D), a clinical marker used to identify luminal and/or intermediate PCa cells. Furthermore, IHC analyses of xenografts from primary PCa cells demonstrated that cells in these xenografts coexpress the prostate-specific marker PSA and the human-specific CD44 isoform (Supplementary Fig. 7E–H).

Importantly, to examine if TICs derived from zebrafish xenografts of primary PCa retain their abilities for serial tumor transplantation, we sorted labeled tumor cells from primary fish xenografts, and used them for secondary xenografts (Fig. 5L). TICs from primary grafts were able to initiate secondary xenografts in 81.8% of cases (n=54/66 secondary xenograft embryo from three patient samples). Thus, PCa xenografts in zebrafish are derived from TICs that can retain genotypic and phenotypic features, some differentiation potential, and serial tumor transplantation ability of human PCa cells, and similar to mouse xenografts, the $\alpha2\beta1^{hi}/CD44^{hi}$ cells are more tumorigenic in zebrafish embryos.

Assessing the frequencies of prostate tumor initiating cells using zebrafish xenografts

TIC frequency of human PCa cells in zebrafish xenografts were determined using ELDA [29] (Supplementary Fig. 8) from SC transplantation of parental, 5-min-adherent $\alpha2\beta1^{hi}/CD44^{hi}$ cells, and 20-min non-adherent $\alpha2\beta1^{low}/CD44^{low}$ cells in limiting dilutions. Self-renewing TICs were found to be abundant, and comprised 0.3–1.3% of DU145 cells (Supplementary Fig. 8) and 0.02–0.9% of PC3 cells.

We also isolated the 5 min-adherent $\alpha2\beta1^{hi}/CD44^{hi}$cells (TICs) from six primary PCa patients (Table 1) from prostatectomies, and examined their tumor initiation potential in zebrafish xenografts. TICs from primary PCa tissues engrafted robustly in the pre-immune

zebrafish embryos at rates higher than that of PCa cell lines (Supplementary Table S3). Self-renewing TICs from primary tumors varied from scarce to widely abundant compared to PCa cell lines, and comprised 0.22% (1/456) to 14.3% (1/7) of primary PCa cells (Table 1).

To study whether the tumorigenic ability of prostate TICs in zebrafish is restricted to transplants in the immune-tolerant embryonic microenvironment, we used prednisone-conditioned juvenile transparent Casper [18] zebrafish as recipients. DU145 parental cells, 5-min-adherent $\alpha 2\beta 1^{hi}$/$CD44^{hi}$ cells, and 20-min non-adherent $\alpha 2\beta 1^{low}$/$CD44^{low}$ cells were transplanted, and fish were monitored at 33°C. Prostate TICs injected SC initiated visible tumors in juvenile fish after an average of 13 days (Supplementary Fig. 9), and then invaded both local and remote tissues by day 28 (Supplementary Fig. 9C). Histological analyses of tumor masses demonstrate cells with engrafted DU145 morphology (Insert in Supplementary Fig. 9B). Whether injected SC in the tail region (Supplementary Fig. 9B–C), or IP (Supplementary Fig. 9D–E), tumors from parental and TIC DU145 cells disseminated to distal sites (Supplementary Table 4). The overall rates of tumor dissemination of 10–500 DU145 cells injected SC and IP in conditioned juvenile fish were 77.8% (n=14/18) with parental cells, 22.2% (n=4/18) with Non-TICs, and 88.8% (n=16/18) with TICs (Supplementary Table 4). Importantly, benign prostate epithelial cells survived but failed to initiate tumors in zebrafish (Supplementary Table 1). Collectively, these data suggest that 5-min-adherent $\alpha 2\beta 1^{hi}$/$CD44^{hi}$ TICs derived from PCa cell lines and primary PCa cells are more tumorigenic in zebrafish xenografts.

DISCUSSION

The presence of distinct subpopulations of TICs in solid tumors has proved contentious [35,36]. However, the evidence for a central role of TICs in tumor growth has most recently been solidified by lineage tracing studies in mice [5–7]. We examined the expression of stem cell markers in multiple PCa cell lines, and found PCa TICs to have increased expression of α2β1-integrin and CD44. We confirmed that TICs derived from primary PCa tissues shared identical properties. We performed several functional assays including colony and serial spheroid formation, migration, and invasion assays, and tumor xenograft studies. We demonstrate that $\alpha 2\beta 1^{hi}$/$CD44^{hi}$ cells robustly adhere to collagen, elevate CD133 reflecting increased abilities to initiate serially-passageable spheres when grown as spheroids, are able to self-renew as single cells in serial spheroid assays, and have enhanced tumor initiation abilities in mice and zebrafish. We identified the rapidly adherent $\alpha 2\beta 1^{hi}$/$CD44^{hi}$ subfraction to consistently contain prostate TICs independent of CD133 expression among all PCa cells that we have examined. Previous studies provided strong evidence for CD133 as a prostate TIC marker [37,38]. Similarly, we have shown here that CD133 expression is elevated in prostate spheres. However, other studies in PCa and other cancers showed tumor initiation independent of CD133 expression [39–42]. The apparent inconsistency of CD133 expression in prostate TICs likely reflects tumor heterogeneity, marker plasticity in response to changes in the niche during PCa clonal evolution, its minute levels (~0.01%), and the necessity for correct CD133 glycosylation and protein folding for precise marking of stem cells [43].

Tumor cells that possess substantial replicative ability might be stem cell-like cells with self-renewing abilities, or mutated transit-amplifying cells without self-renewal capacity [44–46], and the self-renewal states might evolve during the clonal selection process [46]. Multiple molecular pathways regulate the biology of stem cells and self-renewal features, and are therefore potential targets in TICs [47]. Among these reticulate pathways are Bmi-1, Oct3/4, Hedgehog (Hh), Wnt/β-catenin, Notch signaling, Hox gene family, PTEN/Akt pathway, efflux transporters such as ABCG markers of self-renewal, and upregulated telomerase activity [48]. Studies suggest that Bmi-1 is necessary for Hh-[49], and β-catenin-

mediated self-renewal [50] making Bmi-1 one of the most critical self-renewal targets. Thus, the zebrafish xenograft model of tumor initiation that we developed might help to identify inhibitors targeting these critical self-renewal pathways.

Self-renewal is likely a dynamic feature by which cancer cells respond to changes in the microenvironment. Accordingly, the relative frequency of TICs is likely to vary between experimental systems utilizing distinct readouts, microenvironments, and tumor types. We have utilized ELDA, rather than LDA to determine TIC frequencies, since ELDA have the capacity to calculate frequencies for stem cell subpopulations that produce 0% or 100% tumor engraftment [29]. Importantly, we have used zebrafish embryos to develop rapid xenografts of primary PCa cells (within 12 days), and to determine that the frequencies of self-renewing primary PCa cells are more abundant in the immune-permissive zebrafish embryonic microenvironment. Our data provide further evidence for an inverse relationship between the TIC frequency and immune competency of the xenograft recipient [51], and highlight the importance of developing better xenograft models.

Since primary PCa cells are difficult to propagate in mouse xenografts, an approach that is recently adapted in order to increase survival of primary prostate xenografts is tissue recombination of primary PCa cells with inductive stroma [52] by utilizing neonatal mouse mesenchyme [53]. It is increasingly critical to determine if coculture with embryonic heterologous stromal component that promotes epithelial proliferation and differentiation alters the TIC properties of adult prostate epithelial progenitors [54]. Human PCa cells retained many of their phenotypic, differentiation, and serial transplantation features, and displayed metastatic dissemination behavior in zebrafish. Thus, zebrafish xenografts recapitulate a broad spectrum of engrafted PCa cell biology and dissemination behavior, and may be developed to screen for small-molecule inhibitors that target self-renewal to control progression and recurrence of multiple cancers.

Supplementary Material

Refer to Web version on PubMed Central for supplementary material.

Acknowledgments

We thank Dr. Leonard Zon (Harvard) for Casper zebrafish, and Kathleen Flaherty for technical assistance and fish maintenance. This study received funding from Department of Defense Prostate Cancer Grants (W81XWH-12-1-0251 to H.S., J.B., I.K.), and Rutgers Cancer Institute of New Jersey (Pilot Grant to J.B., H.S.).

References

1. Isaacs, JT. Control of cell proliferation and cell deathin the normal and neoplastic prostate: A stem cell model. Rodgers, CHCD.; Cunha, G.; Grayhack, JT.; Hinman, F., Jr; Horton, R., editors. Washington DC: US Department of Health and Human Services; 1987.
2. Isaacs JT, Kyprianou N. Biological basis for chemohormonal therapy for prostatic cancer. Cancer Treat Res. 1989; 46:177–193. [PubMed: 2577189]
3. Collins AT, Berry PA, Hyde C, Stower MJ, Maitland NJ. Prospective identification of tumorigenic prostate cancer stem cells. Cancer Res. 2005; 65(23):10946–10951. [PubMed: 16322242]
4. Dick JE. Stem cell concepts renew cancer research. Blood. 2008; 112(13):4793–4807. [PubMed: 19064739]
5. Chen J, Li Y, Yu TS, McKay RM, Burns DK, Kernie SG, Parada LF. A restricted cell population propagates glioblastoma growth after chemotherapy. Nature. 2012; 488(7412):522–526. [PubMed: 22854781]
6. Driessens G, Beck B, Caauwe A, Simons BD, Blanpain C. Defining the mode of tumour growth by clonal analysis. Nature. 2012; 488(7412):527–530. [PubMed: 22854777]

7. Schepers AG, Snippert HJ, Stange DE, van den Born M, van Es JH, van de Wetering M, Clevers H. Lineage tracing reveals lgr5+ stem cell activity in mouse intestinal adenomas. Science. 2012; 337(6095):730–735. [PubMed: 22855427]
8. Ishii H, Iwatsuki M, Ieta K, Ohta D, Haraguchi N, Mimori K, Mori M. Cancer stem cells and chemoradiation resistance. Cancer Sci. 2008; 99(10):1871–1877. [PubMed: 19016744]
9. Danila DC, Heller G, Gignac GA, Gonzalez-Espinoza R, Anand A, Tanaka E, Lilja H, Schwartz L, Larson S, Fleisher M, Scher HI. Circulating tumor cell number and prognosis in progressive castration-resistant prostate cancer. Clin Cancer Res. 2007; 13(23):7053–7058. [PubMed: 18056182]
10. Patrawala L, Calhoun-Davis T, Schneider-Broussard R, Tang DG. Hierarchical organization of prostate cancer cells in xenograft tumors: The cd44+alpha2beta1+ cell population is enriched in tumor-initiating cells. Cancer Res. 2007; 67(14):6796–6805. [PubMed: 17638891]
11. Berezovska OP, Glinskii AB, Yang Z, Li XM, Hoffman RM, Glinsky GV. Essential role for activation of the polycomb group (pcg) protein chromatin silencing pathway in metastatic prostate cancer. Cell Cycle. 2006; 5(16):1886–1901. [PubMed: 16963837]
12. Choi N, Zhang B, Zhang L, Ittmann M, Xin L. Adult murine prostate basal and luminal cells are self-sustained lineages that can both serve as targets for prostate cancer initiation. Cancer Cell. 2012; 21(2):253–265. [PubMed: 22340597]
13. Tomlins SA, Rhodes DR, Perner S, Dhanasekaran SM, Mehra R, Sun XW, Varambally S, Cao X, Tchinda J, Kuefer R, Lee C, Montie JE, Shah RB, Pienta KJ, Rubin MA, Chinnaiyan AM. Recurrent fusion of tmprss2 and ets transcription factor genes in prostate cancer. Science. 2005; 310(5748):644–648. [PubMed: 16254181]
14. Chaux A, Albadine R, Toubaji A, Hicks J, Meeker A, Platz EA, De Marzo AM, Netto GJ. Immunohistochemistry for erg expression as a surrogate for tmprss2-erg fusion detection in prostatic adenocarcinomas. Am J Surg Pathol. 2011; 35(7):1014–1020. [PubMed: 21677539]
15. Jones PH, Harper S, Watt FM. Stem cell patterning and fate in human epidermis. Cell. 1995; 80(1): 83–93. [PubMed: 7813021]
16. Collins AT, Habib FK, Maitland NJ, Neal DE. Identification and isolation of human prostate epithelial stem cells based on alpha(2)beta(1)-integrin expression. J Cell Sci. 2001; 114(Pt 21): 3865–3872. [PubMed: 11719553]
17. Zon LI, Peterson RT. In vivo drug discovery in the zebrafish. Nat Rev Drug Discov. 2005; 4(1): 35–44. [PubMed: 15688071]
18. White RM, Sessa A, Burke C, Bowman T, LeBlanc J, Ceol C, Bourque C, Dovey M, Goessling W, Burns CE, Zon LI. Transparent adult zebrafish as a tool for in vivo transplantation analysis. Cell Stem Cell. 2008; 2(2):183–189. [PubMed: 18371439]
19. Stoletov K, Montel V, Lester RD, Gonias SL, Klemke R. High-resolution imaging of the dynamic tumor cell vascular interface in transparent zebrafish. Proc Natl Acad Sci U S A. 2007; 104(44): 17406–17411. [PubMed: 17954920]
20. Nicoli S, Ribatti D, Cotelli F, Presta M. Mammalian tumor xenografts induce neovascularization in zebrafish embryos. Cancer Res. 2007; 67(7):2927–2931. [PubMed: 17409396]
21. Marques IJ, Weiss FU, Vlecken DH, Nitsche C, Bakkers J, Lagendijk AK, Partecke LI, Heidecke CD, Lerch MM, Bagowski CP. Metastatic behaviour of primary human tumours in a zebrafish xenotransplantation model. BMC Cancer. 2009; 9:128. [PubMed: 19400945]
22. Quintana E, Shackleton M, Sabel MS, Fullen DR, Johnson TM, Morrison SJ. Efficient tumour formation by single human melanoma cells. Nature. 2008; 456(7222):593–598. [PubMed: 19052619]
23. Patrawala L, Calhoun T, Schneider-Broussard R, Zhou J, Claypool K, Tang DG. Side population is enriched in tumorigenic, stem-like cancer cells, whereas abcg2+ and abcg2− cancer cells are similarly tumorigenic. Cancer Res. 2005; 65(14):6207–6219. [PubMed: 16024622]
24. Xin L, Lawson DA, Witte ON. The sca-1 cell surface marker enriches for a prostate-regenerating cell subpopulation that can initiate prostate tumorigenesis. Proc Natl Acad Sci U S A. 2005; 102(19):6942–6947. [PubMed: 15860580]
25. Croker AK, Goodale D, Chu J, Postenka C, Hedley BD, Hess DA, Allan AL. High aldehyde dehydrogenase and expression of cancer stem cell markers selects for breast cancer cells with

enhanced malignant and metastatic ability. J Cell Mol Med. 2009; 13(8B):2236–2252. [PubMed: 18681906]

26. Tomayko MM, Reynolds CP. Determination of subcutaneous tumor size in athymic (nude) mice. Cancer Chemother Pharmacol. 1989; 24(3):148–154. [PubMed: 2544306]
27. Kramer J, Granier CJ, Davis S, Piso K, Hand J, Rabson AB, Sabaawy HE. Pdcd2 controls hematopoietic stem cell differentiation during development. Stem Cells Dev. 2013; 22(1):58–72. [PubMed: 22800338]
28. Sabaawy HE, Azuma M, Embree LJ, Tsai HJ, Starost MF, Hickstein DD. Tel-aml1 transgenic zebrafish model of precursor b cell acute lymphoblastic leukemia. Proc Natl Acad Sci U S A. 2006; 103(41):15166–15171. [PubMed: 17015828]
29. Hu Y, Smyth GK. Elda: Extreme limiting dilution analysis for comparing depleted and enriched populations in stem cell and other assays. J Immunol Methods. 2009; 347(1–2):70–78. [PubMed: 19567251]
30. Hurt EM, Kawasaki BT, Klarmann GJ, Thomas SB, Farrar WL. Cd44+ cd24(−) prostate cells are early cancer progenitor/stem cells that provide a model for patients with poor prognosis. Br J Cancer. 2008; 98(4):756–765. [PubMed: 18268494]
31. Goldstein AS, Lawson DA, Cheng D, Sun W, Garraway IP, Witte ON. Trop2 identifies a subpopulation of murine and human prostate basal cells with stem cell characteristics. Proc Natl Acad Sci U S A. 2008; 105(52):20882–20887. [PubMed: 19088204]
32. Li A, Simmons PJ, Kaur P. Identification and isolation of candidate human keratinocyte stem cells based on cell surface phenotype. Proc Natl Acad Sci U S A. 1998; 95(7):3902–3907. [PubMed: 9520465]
33. Shinohara T, Orwig KE, Avarbock MR, Brinster RL. Spermatogonial stem cell enrichment by multiparameter selection of mouse testis cells. Proc Natl Acad Sci U S A. 2000; 97(15):8346–8351. [PubMed: 10900001]
34. Vazquez-Martin A, Oliveras-Ferraros C, Del Barco S, Martin-Castillo B, Menendez JA. The anti-diabetic drug metformin suppresses self-renewal and proliferation of trastuzumab-resistant tumor-initiating breast cancer stem cells. Breast Cancer Res Treat. 2010; 126(2):355–364. [PubMed: 20458531]
35. Visvader JE, Lindeman GJ. Cancer stem cells in solid tumours: Accumulating evidence and unresolved questions. Nat Rev Cancer. 2008; 8(10):755–768. [PubMed: 18784658]
36. Rosen JM, Jordan CT. The increasing complexity of the cancer stem cell paradigm. Science. 2009; 324(5935):1670–1673. [PubMed: 19556499]
37. Vander Griend DJ, Karthaus WL, Dalrymple S, Meeker A, DeMarzo AM, Isaacs JT. The role of cd133 in normal human prostate stem cells and malignant cancer-initiating cells. Cancer Res. 2008; 68(23):9703–9711. [PubMed: 19047148]
38. Richardson GD, Robson CN, Lang SH, Neal DE, Maitland NJ, Collins AT. Cd133, a novel marker for human prostatic epithelial stem cells. J Cell Sci. 2004; 117(Pt 16):3539–3545. [PubMed: 15226377]
39. Taylor RA, Toivanen R, Frydenberg M, Pedersen J, Harewood L, Collins AT, Maitland NJ, Risbridger GP. Australian Prostate Cancer B. Human epithelial basal cells are cells of origin of prostate cancer, independent of cd133 status. Stem Cells. 2012; 30(6):1087–1096. [PubMed: 22593016]
40. Zhou J, Wang H, Cannon V, Wolcott KM, Song H, Yates C. Side population rather than cd133(+) cells distinguishes enriched tumorigenicity in htert-immortalized primary prostate cancer cells. Mol Cancer. 2011; 10:112. [PubMed: 21917149]
41. Pfeiffer MJ, Schalken JA. Stem cell characteristics in prostate cancer cell lines. Eur Urol. 2009; 57(2):246–254. [PubMed: 19200636]
42. Pellacani D, Packer RJ, Frame FM, Oldridge EE, Berry PA, Labarthe MC, Stower MJ, Simms MS, Collins AT, Maitland NJ. Regulation of the stem cell marker cd133 is independent of promoter hypermethylation in human epithelial differentiation and cancer. Mol Cancer. 2011; 10:94. [PubMed: 21801380]

43. Pellacani D, Oldridge EE, Collins AT, Maitland NJ. Prominin-1 (cd133) expression in the prostate and prostate cancer: A marker for quiescent stem cells. Adv Exp Med Biol. 2013; 777:167–184. [PubMed: 23161082]
44. Hemmati HD, Nakano I, Lazareff JA, Masterman-Smith M, Geschwind DH, Bronner-Fraser M, Kornblum HI. Cancerous stem cells can arise from pediatric brain tumors. Proc Natl Acad Sci U S A. 2003; 100(25):15178–15183. [PubMed: 14645703]
45. Singh SK, Clarke ID, Terasaki M, Bonn VE, Hawkins C, Squire J, Dirks PB. Identification of a cancer stem cell in human brain tumors. Cancer Res. 2003; 63(18):5821–5828. [PubMed: 14522905]
46. Nowell PC. The clonal evolution of tumor cell populations. Science. 1976; 194(4260):23–28. [PubMed: 959840]
47. Mimeault M, Batra SK. Frequent gene products and molecular pathways altered in prostate cancer-and metastasis-initiating cells and their progenies and novel promising multitargeted therapies. Mol Med. 2011; 17(9–10):949–964. [PubMed: 21607288]
48. Reya T, Morrison SJ, Clarke MF, Weissman IL. Stem cells, cancer, and cancer stem cells. Nature. 2001; 414(6859):105–111. [PubMed: 11689955]
49. Liu S, Dontu G, Mantle ID, Patel S, Ahn NS, Jackson KW, Suri P, Wicha MS. Hedgehog signaling and bmi-1 regulate self-renewal of normal and malignant human mammary stem cells. Cancer Res. 2006; 66(12):6063–6071. [PubMed: 16778178]
50. Bisson I, Prowse DM. Wnt signaling regulates self-renewal and differentiation of prostate cancer cells with stem cell characteristics. Cell Res. 2009; 19(6):683–697. [PubMed: 19365403]
51. O'Brien CA, Kreso A, Jamieson CH. Cancer stem cells and self-renewal. Clin Cancer Res. 2010; 16(12):3113–3120. [PubMed: 20530701]
52. Goldstein AS, Drake JM, Burnes DL, Finley DS, Zhang H, Reiter RE, Huang J, Witte ON. Purification and direct transformation of epithelial progenitor cells from primary human prostate. Nat Protoc. 2011; 6(5):656–667. [PubMed: 21527922]
53. Toivanen R, Berman DM, Wang H, Pedersen J, Frydenberg M, Meeker AK, Ellem SJ, Risbridger GP, Taylor RA. Brief report: A bioassay to identify primary human prostate cancer repopulating cells. Stem Cells. 2011; 29(8):1310–1314. [PubMed: 21674698]
54. Risbridger GP, Taylor RA. Minireview: Regulation of prostatic stem cells by stromal niche in health and disease. Endocrinology. 2008; 149(9):4303–4306. [PubMed: 18535102]

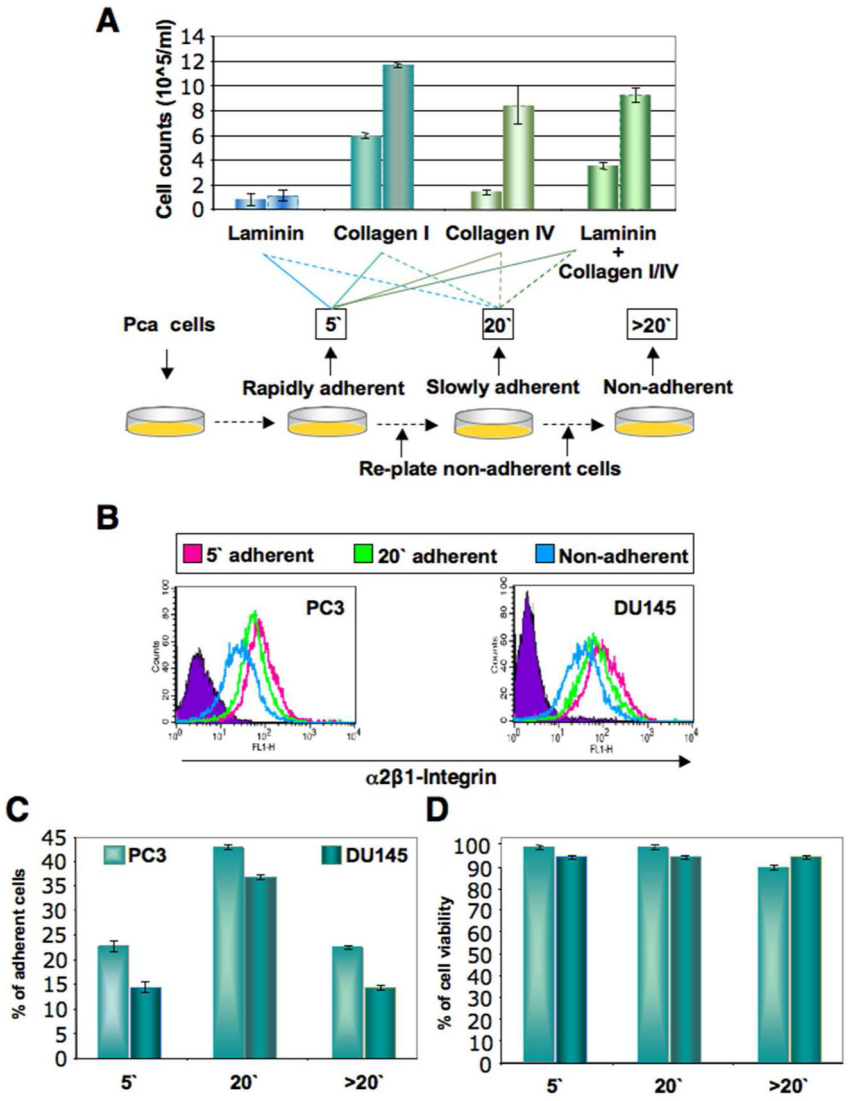

Fig 1.

Isolation of subpopulations of prostate cancer cells by differential adherence. **A**: Multiple prostate cancer cell lines were allowed to adhere to either laminin-, collagen I-, collagen IV-coated plates, or plates coated with all three combinations. Time of adherence assay is described where PCa cells are allowed to adhere for 5 minutes, the rapidly adherent cells after 5 min (5′) are collected, the remaining of the cells are replated for 20 min, the cells that adhere at 20 min (20′) are collected, and the cells that did not adhere (>20′) are labeled as non-adherent cells. Data are shown for DU145 cells from six separate adhesion experiments. **B**: Fractions of PC3 and DU145 cells collected after time-of-adherence assay were subjected to flow cytometric analysis of α2β1-integrin expression. Representative flow cytometric analysis is shown for PC3 and DU145 cells. **C**: Percentages of collagen-I adherent and non-adherent PC3 and DU145 cells immediately after collagen adherence assay. **D**: Cell viability of collagen-I adherent and non-adherent PC3 and DU145 cells immediately after the collagen adherence assay were similar to cell viabilities of adherent and non-adherent cells immediately after cell isolation, and averaged 95–99.9%.

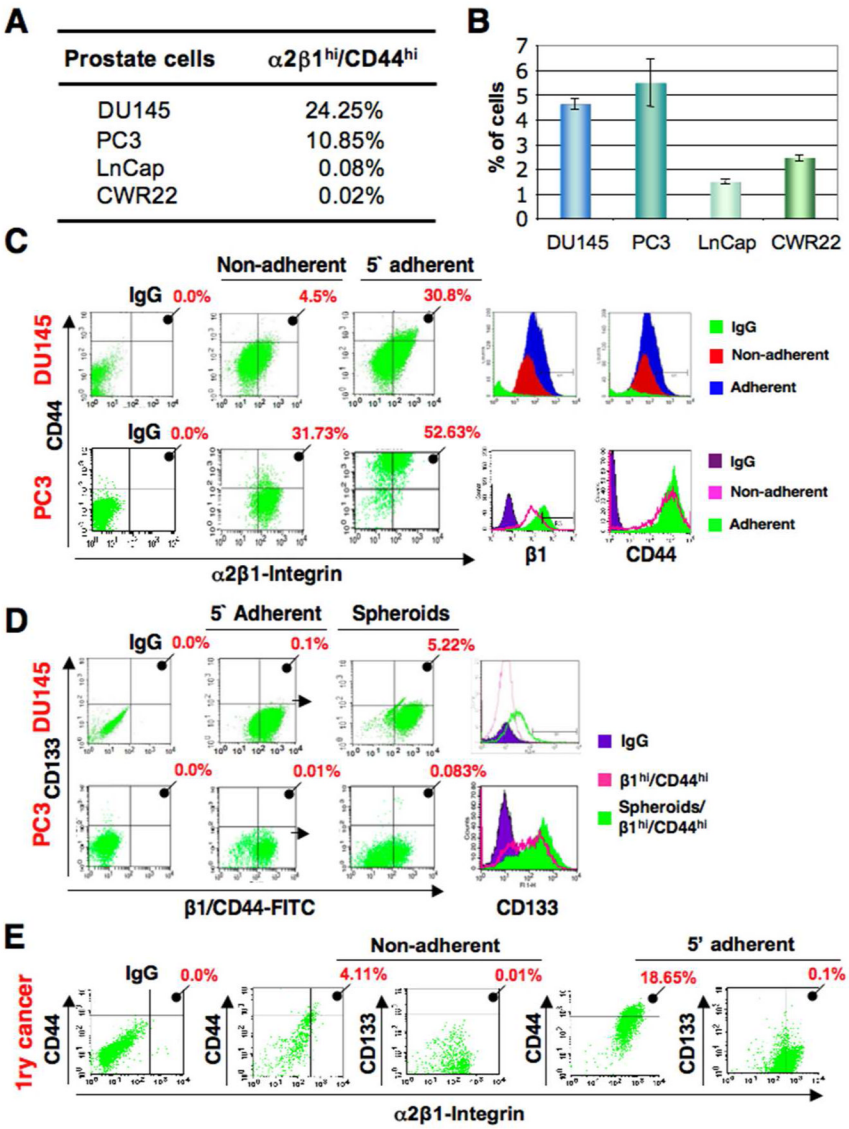

Fig 2.

Collagen-adherent cells are enriched in putative TICs. **A**: Mean percentage of cells with $\alpha2\beta1^{hi}/CD44^{hi}$ phenotype in PCa cell lines. **B**: Time-of-adherence assay performed on multiple PCa cell lines displaying the 5-min adherent cell fraction as a percentage of total cells. Data represent three independent experiments performed in triplicates. **C**: Flow cytometric analyses of DU145 and PC3 cells after collagen adherence showing both increased expression of CD44 and CD133 in the 5-min (5′) adherent cells compared to the 20 minutes (20′) non-adherent cells, and higher mean fluorescence intensity (MFI) of 5 minutes collagen-I-adherent ($\alpha2\beta1^{hi}/CD44^{hi}$) cells (Adherent) compared to 20 min-non-adherent ($\alpha2\beta1^{low}/CD44^{low}$) cells (Non-adherent), and IgG control (IgG). **D**: CD133 expression in various subsets of DU145 and PC3 cells. In a representative experiment, $\alpha2\beta1^{hi}/CD44^{hi}$ (pink) showed 0.1% and 0.01% of the cells positive for CD133 from DU145 and PC3 cells respectively, and spheroids from these $\alpha2\beta1^{hi}/CD44^{hi}$ cells (green) showed upregulated CD133 levels up to 5.22% in DU145 cells and 0.083% in PC3 cells ($P< 0.001$ for both cell lines in three independent experiments). **E**: Primary prostate cancer cells have increased expression of CD44 and CD133 in the 5-min adherent cells compared to the 20

min-non-adherent cells. Mean percentages from analyses of six cases are displayed. Higher expression of α2β1/CD44 and upregulation of CD133 when cells are grown as spheres were detected in the 5-min adherent cells compared to the 20 minutes non-adherent cells, and were seen with all six patient samples examined.

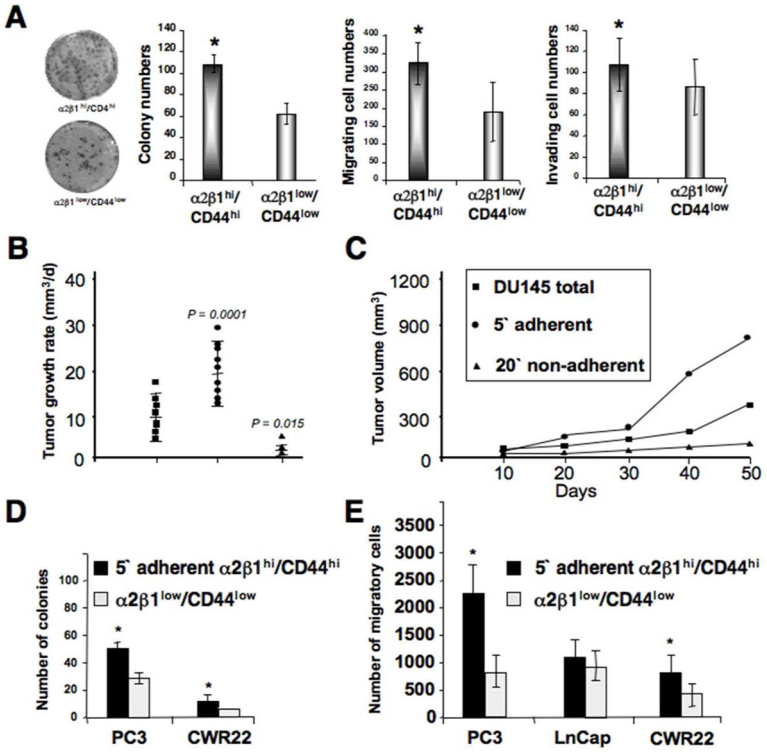

Fig 3.

Tumorigenic potential of collagen-adherent $\alpha2\beta1^{hi}/CD44^{hi}$ cells. **A**: The two fractions of $\alpha2\beta1^{hi}/CD44^{hi}$ cells and $\alpha2\beta1^{low}/CD44^{low}$ cells isolated after collagen adherence were assessed in colony forming efficiency assays. Images on the left demonstrate colonies derived from both fractions stained with crystal violet. Numbers of spheroid colonies, migrating, and invading cells are displayed as mean ± SD, and were done in triplicates. Self-renewal and in vitro tumorigenic potential of collagen-adherent $\alpha2\beta1^{hi}/CD44^{hi}$ DU145 cells are shown. Bars demonstrate the enhanced clonogenic ability of $\alpha2\beta1^{hi}/CD44^{hi}$ cells compared to $\alpha2\beta1^{low}/CD44^{low}$ cells. The two fractions of $\alpha2\beta1^{hi}/CD44^{hi}$ cells and $\alpha2\beta1^{low}/CD44^{low}$ DU145 cells isolated after collagen adherence were assessed for numbers of migrating cells. Data are displayed as mean ± SD, and were done in triplicates (*$p<0.001$). **B**: Both flanks of athymic nude ($NCI^{nu/nu}$) mice were injected with either total DU145 cells (ν), 5 min-adherent cells (λ), or 20 min-non-adherent cells (σ) (n=60 mice). Mean tumor growth rates are presented as mm^3/day ± SD. **C**: The mean tumor volume was plotted as a function of time using the ellipsoid volume formula (length x $width^2$ x 1/2), assuming $\pi = 3$. P values shown are compared with total DU145 tumors. D–E: Self-renewal and *in vitro* tumorigenic potential of collagen-adherent $\alpha2\beta1^{hi}/CD44^{hi}$ PC3, LnCap and CWR22 PCa cells. **D**: Bars demonstrate the enhanced clonogenic ability of $\alpha2\beta1^{hi}/CD44^{hi}$ cells compared to $\alpha2\beta1^{low}/CD44^{low}$ PC3 and CWR22 cells. **E**: The two fractions of $\alpha2\beta1^{hi}/CD44^{hi}$ cells and $\alpha2\beta1^{low}/CD44^{low}$ PC3, LnCap and CWR22 cells isolated after collagen adherence were assessed for numbers of migrating cells. Data are displayed as mean ± SD, and were done in triplicates (*$p<0.001$).

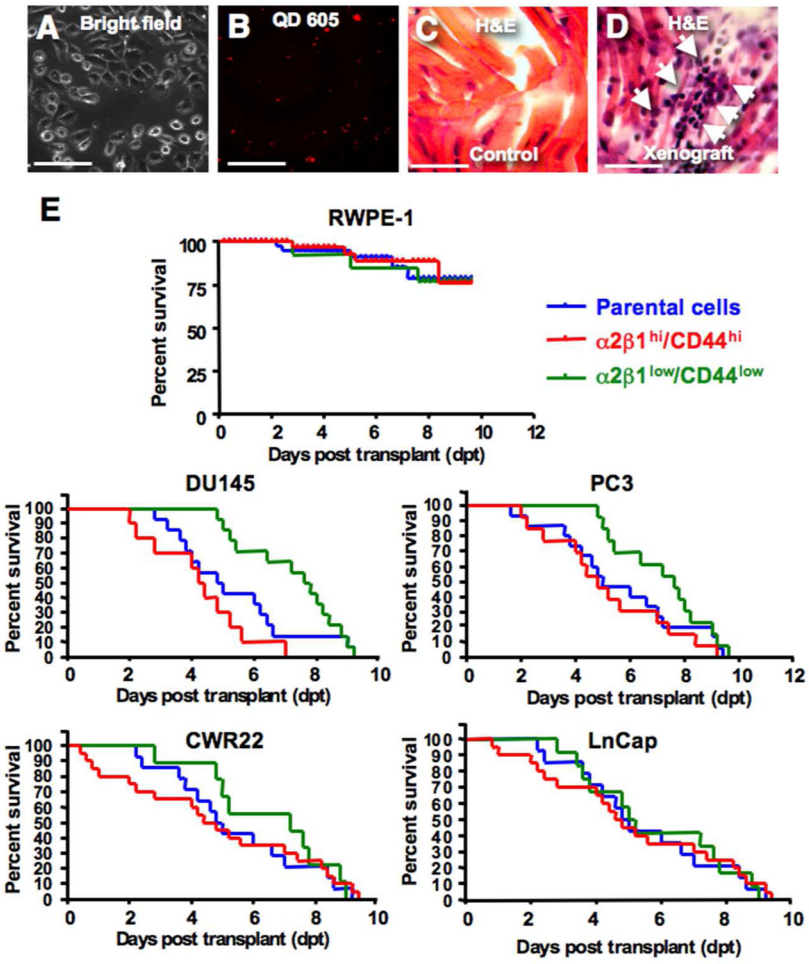

Fig. 4.

Zebrafish xenografts of human prostate cancer cells. **A**–**D**: Bright filed image in (A), and the corresponding red (605) fluorescent image in (**B**) demonstrating efficient labeling of DU145 cells with quantum dots-605 (QD) in nearly all the cells in the field. **C**–**D**: Histological H&E sections from a control non-transplanted zebrafish muscle tissues in (**C**), compared to a muscle section from DU145 TICs transplanted fish in (**D**). Section demonstrates tumor infiltrates with cells resembling morphology of DU145 cells in fish tissues. Scale bar is 100 μM in (**A**–**D**). **E**: Kaplan Meier survival curve of embryos transplanted with normal prostate cells and multiple PCa cells lines using three fractions; parental (blue), 5′ adherent $\alpha 2\beta 1^{hi}$/$CD44^{hi}$ cells (TICs) (red), and 20-min non-adherent $\alpha 2\beta 1^{low}$/$CD44^{low}$ (green) cells. Embryos transplanted with cancer cells had significantly shorter survival rates compared to normal prostate cells due to the rapid development of disseminated tumors. The TICs fraction induced significantly higher mortality rates from tumor growth with DU145, PC3 and CWR22 but not LnCap cells when compared to parental and non-TICs transplants.

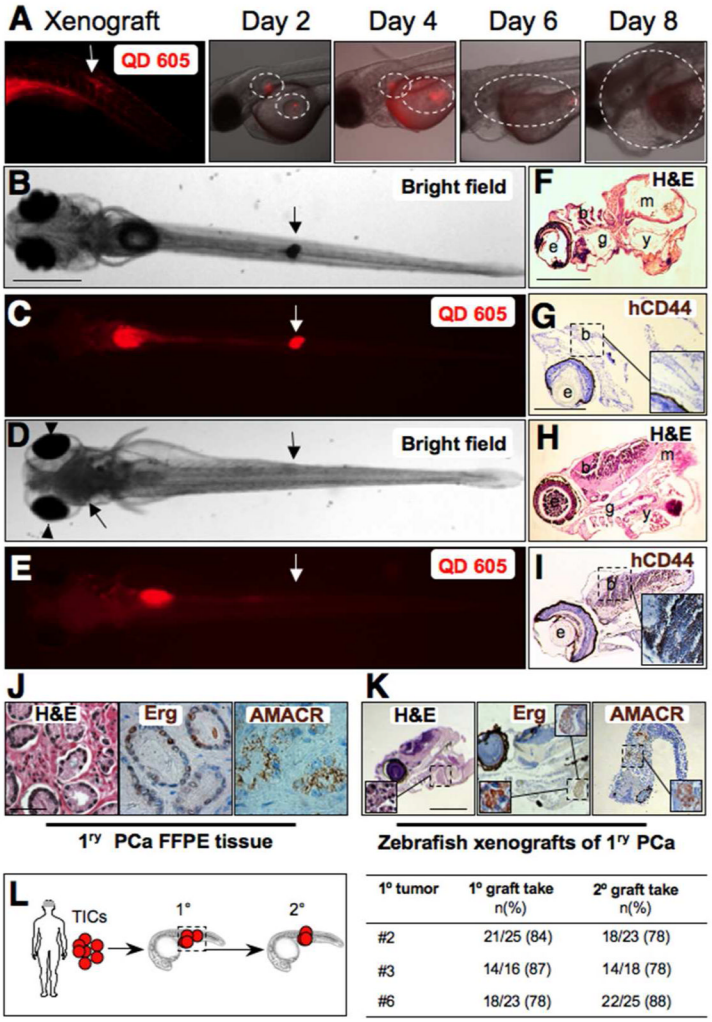

1° tumor	1° graft take n(%)	2° graft take n(%)
#2	21/25 (84)	18/23 (78)
#3	14/16 (87)	14/18 (78)
#6	18/23 (78)	22/25 (88)

Fig. 5.

Prostate cancer xenograft tumor progression in zebrafish. **A**: QD 605 red fluorescent image of the site of injection on the left taken on the same day of transplanting primary PCa cells SC in zebrafish embryos. Red and bright image overlays represent sequential imaging of the same xenograft embryo over time during 8 days of tumor growth. From day 2, notice the two sites that are outlined with tumor cells labeled with QD. Tumor growth increases progressively while fluorescence decreases due to QD dilution with cell division. **B**–**E**: Sections from control and PCa xenografts with brain metastasis (**D**–**E**). Images were taken at 9 dpt. Downward arrows indicate the site of SC transplantation. Upward arrows in **D** and **E** on the left indicate cell masses invading the brain and causing exophthalmus (arrowheads in **D**, compare with no brain metastasis in **B**). **F**–**K**, H&E staining (**F** and **H**) and IHC with anti-human CD44 (**G** and **I**) in a representative control untransplanted embryo (**F**–**G**) compared to histological sections from a representative xenotransplanted embryo (**H**–**I**) with brain metastasis stained with H&E (**H**) and IHC staining of the same brain region containing disseminated human cells identified with the human isoform-specific anti-CD44 antibody (Insert) (**H,I**). Letters indicate e, eye; b, brain; m, muscle; y, yolk. Inserts in panels **G** and **I** are higher magnification of the outlined brain areas, respectively. **J**: Formalin fixed paraffin embedded (FFPE) sections from a representative primary prostate cancer (PCa) tissue used that are stained with H&E, or in IHC with either Erg or AMACR in brown. The H&E image

in **J** is a higher magnification of the outlined areas in supplementary Fig. 4C, while The Erg and AMACR images in **J** are higher magnifications of the outlined areas in supplementary Fig. 6H and 5F, respectively. **K**: Sections from zebrafish embryo with PCa xenograft using cells from tissues shown in Fig. 5K and stained with H&E, and IHC for Erg and AMACR. Inserts are higher magnification of the outlined area in **K. L**: Diagram demonstrating strategy to study tumor initiation potential of primary PCa cell grafts in secondary xenografts. TICs from the 5-min adherent $\alpha 2\beta 1^{hi}$/$CD44^{hi}$ cells of three patient samples #4, #5, and #6 were transplanted to generate primary xenografts (1°). Xenograft tumor areas were dissected, pooled, and TICs were sorted and injected into secondary recipients. Table on the right demonstrates primary and secondary graft take rates. Scale bars are 100 μm in **B**–**E**, **F**–**J**, and **N**–**K**.

Table 1

TIC frequencies of cells from primary prostate cancer patients in zebrafish xenografts.

1^{ry} prostate	Gleason	R2	99% confidence	TIC frequency
1	3 + 3	0.999	1/7 to 1/37	1/16
2	3 + 3	0.995	1/29 to 1/153	1/71
3	3 + 3	0.995	1/64 to 1/228	1/120
4	3 + 3	0.999	1/59 to 1/456	1/185
5	3 + 3	0.995	1/32 to 1/114	1/36
6	3 + 4	0.998	1/29 to 1/153	1/71

Table shows patient number and Gleason scores. TIC frequencies of 1/16 (6.25%), 1/71 (1.4%), 1/120 (0.83%), 1/185 (0.54%), 1/36 (2.7%), 1/71 (1.4%), 1/8 (12.5%), 1/16 (6.25%), and a frequency range of 0.22% to 25.0% were calculated in the six patient samples using ELDA with 99% confidence interval, and with the displayed correlation coefficient (R2) values. Fifty embryos per dilution per tumor sample were transplanted SC with limiting dilution (3–100 cells) of TICs from the 5-min adherent $\alpha 2\beta 1^{hi}/CD44^{hi}$ cells. Tumor cell graft take was consistently high, and averaged 77 ± 10%, and embryo survival next day after transplantation was >86%.